This article has been accepted for publication in IEEE Internet of Things Journal. This is the author's version which has not been fully edited and content may change prior to final publication. Citation information: DOI 10.1109/JIOT.2023.3327883

TDOA-based Indoor Localization via Linear Fusion with Low-Rank Matrix Approximation

Haibin Li, *Student Member, IEEE,* Osama Elnahas, *Member, IEEE,* and Zhi Quan, *Senior Member, IEEE*

***Abstract*—Target indoor localization has become an attractive research topic due to its importance in location-based applications in wireless networks for sensing, controlling, and communicating. In TDOA-based localization models, timestamp packets must be exchanged between anchor nodes and target nodes. Timestamp measurements are susceptible to random transmission delays and packet loss in indoor environments, resulting in inaccurate positioning accuracy. In this paper, we propose a linear fusion indoor localization scheme based on TDOA with low-rank approximation to improve target localization accuracy and robustness. In an asynchronous localization model, we first formulate the indoor localization problem from incomplete and noisy timestamp measurements as a low-rank matrix completion problem. Furthermore, the proposed linear fusion algorithm is used to further optimize the localization accuracy by weighting multiple localization rounds. Simulation and experimental results indicate that the proposed method is more effective than the existing methods in the presence of packet loss and random delays.**

***Index Terms*—Localization, time-difference-of-arrival (TDOA), matrix completion, linear fusion.**

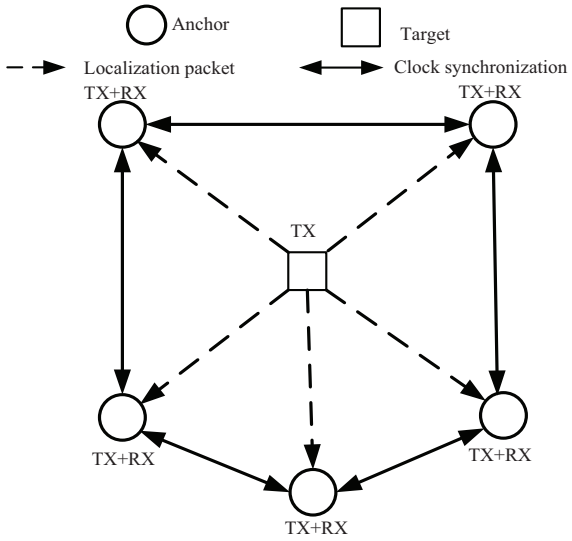

Fig. 1: Traditional TDOA measurement method.

I. Introduction

Target localization has emerged as a promising solution to communicate, sense, and control robotic systems, especially in industrial settings with advancements in wireless technology [1], [2]. It is essential for the proper operation of such applications to have precise target location information. With its global coverage, the Global Positioning System (GPS) is an excellent localization system for outdoor applications. As a result of multipath fading and signal attenuation, GPS is not an appropriate solution for indoor applications. The majority of Internet of Things (IoT) scenarios occur within an indoor environment, and these IoT technologies can be used to enhance indoor location awareness in a variety of ways [3], [4]. In recent years, ultra-wideband (UWB) technology has been proposed as a technique for indoor localization. Models using UWB have low power consumption, high data transfer rates, and nanosecond timestamps [5], [6].

Indoor localization can be classified into two categories: range-based and range-free. Range-free localization methods do not require additional hardware for absolute point-to-point distance measurements, but have higher localization errors. Range-based localization methods have been extensively investigated in the literature, including signal strength (RSS), direction of arrival (DOA), time of arrival (TOA), time difference of arrival (TDOA), and angle of arrival (AOA), etc [7], [8]. TDOA is the most popular method due to its low cost, accuracy, and simplicity [7], [9].

TDOA-based target localization involves the following steps. First, the anchor nodes are synchronized to a common time reference as shown in Fig.1. Next, the measured time difference between a target node and a spatially distributed anchor node is used to determine a hyperbolic model. By intersecting the calculated TDOA values with numerous hyperbolas, the target node can be located [7].

Reliable clock synchronization between all anchor nodes is essential to the design of TDOA localization methods. However, even if all clocks in the network are synchronized accurately, they may drift away from each other over time due to oscillator imperfections and other environmental factors. It is possible for target localization errors to be significant if there is a small difference between the network clocks [10]. Therefore, each node needs to be synchronized periodically. Numerous clock synchronization methods have been proposed in wireless networks, including Timing Synch Protocol for Sensor Networks (TPSN), Flooding Time Synchronization Protocol (FTSP), and Reference Broadcast Synchronization (RBS) [11]. Traditionally, clock-synchronization-based localization models have relied on a large number of packet exchanges between anchor nodes to achieve high-accuracy localization at the cost of communication overhead and system complexity [12]. As a result, these synchronization-based methods are extremely challenging for high-accurate localization.

H.B. Li, Osama Elnahas, and Z. Quan are with the College of Electronics and Information Engineering, Shenzhen University, Shenzhen, China 518060. (*Corresponding Author: Zhi Quan*. E-mails: 2050432005@szu.edu.cn; osama@szu.edu.cn; zquan@szu.edu.cn).

Osama Elnahas is with the Department of Electrical Engineering, Faculty of Engineering, Assiut University, Egypt, and with the Faculty of Industry and Energy Technology, Borg Al-Arab Technological University, Egypt.

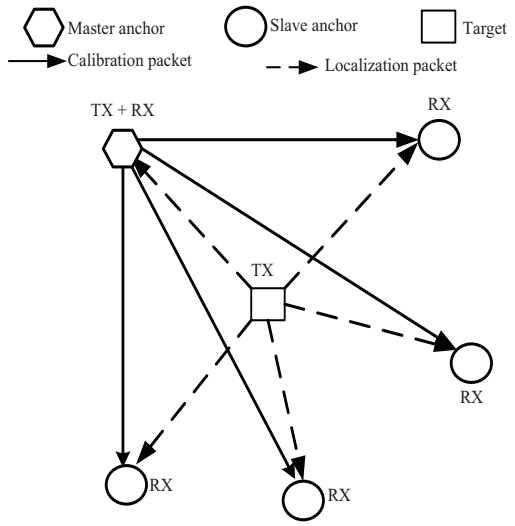

Fig. 2: Asynchronous TDOA measurement method.

In the past few years, a few localization methods have been proposed to measure the TDOA directly without synchronization. [13]–[15]. In [16], the ASync-TDOA localization model uses a reference node to obtain TDOA measurements without anchors synchronizing their clocks as shown in Fig. 2. With this one-way-based ranging model, packet exchanges can be reduced and a high level of accuracy can be achieved at a relatively low cost. In this paper, we use UWB signals to collect timestamps and the ASync-TDOA to measure TDOAs.

A. Related Work and Motivation

Recently, indoor target localization has attracted considerable attention due to the increasing demand for location-based services. A major advantage of UWB technology is its high time resolution and high bandwidth, which makes it an attractive choice for high-precision indoor localization. Localization models based on UWB use very short-duration pulses on the order of nanoseconds, which minimize multipath effects and provide accurate Time of Flight (TOF) estimations. Thus, UWB technology is particularly suitable for range-based approaches such as TDOA localization models. Several localization systems have used UWB to localize objects, with encouraging results.

There are many factors that influence the TDOA measurements in UWB localization models, such as anchor node positions, clock synchronization, random transmission delays, and packet loss. In [17], the authors analyzed how anchor position errors affect target location accuracy. In order to improve localization accuracy, they proposed an algorithm with a closed-form solution based on the statistical distribution of anchor positions. The study in [18] considered using a single calibration emitter with a precisely known location to reduce the loss in target localization accuracy caused by the random anchor position errors. These approaches could reach the Cramer-Rao lower bound (CRLB) when anchor position errors are sufficiently small at the cost of increased computational complexity.

Significant research efforts in indoor target localization have focused on precise synchronization for TDOA measurements [19]. In [10], the authors studied TDOA-based indoor target localization in the presence of clock imperfections. This study presented joint clock skew and target location estimation based on semidefinite programming with a refining step. Moreover, differential TDOA is proposed in [20], [21] as a method for mitigating the effects of imperfect clocks by employing a nonlinear least squares criterion. In [11], the authors develop a robust maximum likelihood estimator for the clock skew and clock offset in order to achieve high synchronization accuracy. The method developed in [22] uses wireless clock synchronization based on IEEE 802.15.4a for TDOA-based localization. A high-precision TDOA positioning scheme is proposed in [23] based on IEEE 802.15.4z. The authors in [24] designed transmitter and receiver boards for localization using clock offset estimation. A asymptotic gradient clock synchronization algorithm is proposed in [25], which relies on periodic transmissions from each node to correct clock bias and gradually approaches global clock consistency. In spite of the fact that these synchronized localization models have very good accuracy, their synchronization method is quite complex and increases network load.

The author proposes a coherent integration TDOA estimation method that minimizes time synchronization errors by using the target and reference signals [26]. It is actually difficult for the receiver to guarantee the same random phase between signals received from mixers and receivers in different frequency bands simultaneously.

Various approaches have been developed in recent years to calculate the TDOA measurements without synchronization. Based on two-signal sensing and sample counting techniques in [27], the author proposes a novel TDOA localization technique without clock synchronization. The TDOA method proposed in [28] is capable of measuring the time difference without the need for clock synchronization, but it requires the initial coordinates of the target node. Asynchronous hyperbolic source localization is proposed in [29], which relies on packet exchange between two anchors to reduce errors caused by clock drift. An algorithm for one-way transmission ranging has been proposed in [30] that does not require clock synchronization between anchors, but requires each anchor to send a broadcast packet to estimate and compensate for clock offsets. In [16], the authors presented an asynchronous TDOA method that uses a reference node to determine the time difference between anchor and target nodes. The proposed method is implemented on a localization platform with UWB signals to estimate the target node's position.

In the above-mentioned literature, since the TDOA measurements are calculated based on localization timestamps received by the server from the anchor nodes, very precise timestamps are required to estimate the target location. Most of the existing TDOA-based localization algorithms in the literature calculate the TDOA measurements directly using the noisy timestamps collected with the assumption that full localization timestamps have been received. However, in practical wireless communication networks, the received timestamps can be affected by delay variations and thereby degrade the localization process. Credible target position estimation is challenged by the transmission delay of the timestamp packets. Transmission delays

can be divided into two types: fixed delays and random delays. In addition, limited communication range, and environmental effects result in timestamp packet loss that affects the accuracy of localization. Target localization is adversely affected by the loss of timestamp packets, and the performance deteriorates even further in harsh wireless environments when successive packet loss occurs. Thus, the noisy and incomplete timestamps must be processed before TDOA calculations are performed.

Motivated by the above-mentioned challenges, in this paper, we develop a robust TDOA localization algorithm based on low-rank matrix approximation. The LRMA localization scheme is able to correct the received timestamps in the presence of random transmission delays and missing data, resulting in improved target localization. The proposed algorithm has two complementary stages. In the first stage, the timestamp correction problem is formulated as a low-rank matrix completion problem arising from a noisy and incomplete timestamp matrix. The purpose of timestamp correction and recovery is to reconstruct the original timestamps from their noisy, incomplete received set as accurately as possible. In order to overcome the nonconvexity of the rank minimization problem, we show that this problem can be solved by minimizing the nuclear norm of the matrix as convex relaxation. To improve the estimation accuracy, the second stage uses a linear fusion algorithm to estimate the target location based on the recovered timestamps.

B. Main Contributions

We propose a linear fusion algorithm for TDOA localization with noisy and incomplete timestamps that utilizes a low-rank matrix completion algorithm. The TDOA measurements are calculated directly based on the received timestamps between the anchor nodes and target nodes using the ASync-TDOA model. The main contributions of this paper are summarized as follows:

- We propose a framework for indoor localization based on TDOA under random loss of timestamp packets. With the collected set of timestamp packets, we develop a rank-two matrix model. The formulated timestamp matrix consists of rows that represent the localization rounds of anchor nodes, and columns representing their timestamps.
- We formulate the localization problem from a noisy and incomplete timestamp matrix into a low-rank matrix recovery problem using the known subset of timestamp information. The proposed scheme first solves the formulation recovery problem by minimizing the Frobenius norm. Secondly, using the recovered timestamps, the proposed scheme calculates TDOA measurements between the target node and the known anchors, and then estimates the location of the target.
- We devise a linear fusion strategy based on the collected set of localization rounds in order to improve positioning accuracy further.

The experimental results show that the proposed scheme is more accurate than state-of-the-art methods under conditions of timestamp packet loss and corruption.

The rest of the paper is structured as follows. We review the preliminary in Section II. Section III introduces the proposed matrix completion-based target localization method, including timestamp matrix formulation, timestamp matrix recovery strategy, and traditional localization algorithms. We optimize the localization results using the linear weighted fusion algorithm in Section IV. In Section V, the performance improvement of the proposed localization algorithm is verified by simulation results. Additionally, we verify the algorithm's effectiveness in hardware experiments in Section VI. Finally, we summarize the paper in Section VII.

II. Preliminaries

A. TDOA Localization Model

In the traditional TDOA measurement method, the working principle of a group of anchor nodes is shown in Fig.2. Consider an array of $N \geq 4$ anchor nodes in 3-dimensional space. We define $P = (x, y, z)^T$ as the unknown coordinates of the target node and $P_i = (x_i, y_i, z_i)^T, i = 1, 2, \cdots, N$ as the known coordinates of the i-th anchor node. Generally, we refer to the first anchor node as the master anchor, and the remaining anchor nodes as the slave anchors. The TDOA measurements between the master anchor and the i-th slave anchor are denoted by

$$\tilde{t}_{i,1} = \tilde{t}_i - \tilde{t}_1, i = 2, 3, \cdots, N, \tag{1}$$

where $\tilde{t}_i$ is the real-time of signal propagation between the target node and the i-th anchor node.

In traditional TDOA technologies, precise clock synchronization between anchor nodes is required to be maintained. A large number of timestamp packets need to be exchanged regularly between anchor nodes to synchronize clocks, which increases estimation and network overhead [31]. Additionally, clock skew and drift make it difficult to precisely solve the problem of clock synchronization. To reduce packet exchanges, we considers a TDOA localization method based on an asynchronous network [32]. It is possible to measure TDOAs using this calibration packet-based model without clock synchronization.

As shown in Fig. 3, the TDOA measurement process involves the following steps:

1) The master anchor records the current time t_k^M, and then broadcasts a calibration packet to all slave anchors.
2) The i-th slave anchor records the time of receiving the master calibration packet with their local clock $t_k^{S_{i,M}}$.
3) Target node broadcasts the localization packet.
4) The i-th slave anchor records the time of receiving the localization packet with their local clock $t_k^{S_{i,T}}$, and the master anchor records the time of receiving this localization packet with its local clock $t_k^{M,T}$.
5) Repeat the above steps $J \geq 10$ times to get a set of timestamps $\boldsymbol{T}_s$ with J rows.

We can calculate all TDOA measurements based on the collection set of timestamps, which is denoted as $\boldsymbol{T}_s = \left\{ t_k^M, t_k^{S_1,M}, \ldots, t_k^{S_{N-1},M}, t_k^{M,T}, t_k^{S_1,T}, \ldots, t_k^{S_{N-1},T} \right\}_{k=1}^{J}$.

This article has been accepted for publication in IEEE Internet of Things Journal. This is the author's version which has not been fully edited and content may change prior to final publication. Citation information: DOI 10.1109/JIOT.2023.3327883

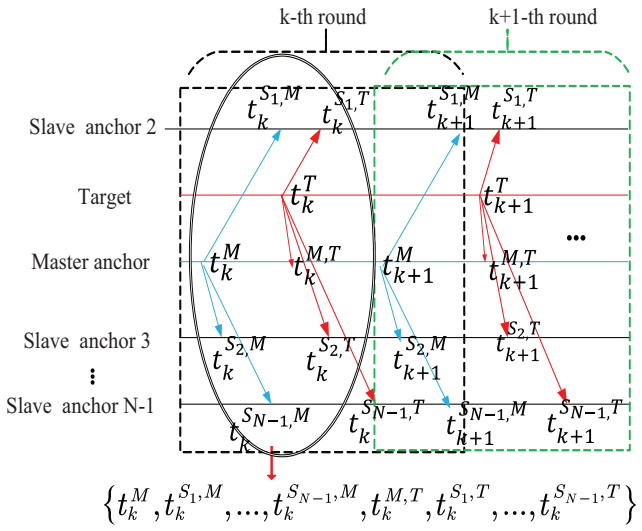

Fig. 3: TDOA measurement process.

To calculate the TDOA value without clock synchronization, $t_k^{S_i,T}$ are mapped to the clock of master anchor [16], which is denoted by

$$t_k^{S_i,T} \overset{\text{mapping}}{\Rightarrow} t_k^{S_i,T,M}. \tag{2}$$

With the location of anchor nodes known, the time of flight from the master anchor to the i-th slave anchor can be determined. As a result, $t_k^{S_i,T,M}$ can be calculated by

$$\frac{t_k^{S_i,T,M} - t_k^M - \Delta t_{M,S_i}}{t_{k+1}^M - t_k^M} = \frac{t_k^{S_i,T} - t_k^{S_i,M}}{t_{k+1}^{S_i,M} - t_k^{S_i,M}}, \tag{3}$$

where $\Delta t_{M,S_i}$ represents the time of flight from the master anchor to the i-th slave anchor. Finally, the TDOA measurements between master node and i-th slave node, denoted as T_k^{M,S_i}, is given by

$$T_k^{M,S_i} = t_{\mathrm{k}}^{M,T} - t_k^{S_i,T,M}. \tag{4}$$

B. Matrix Completion

In signal processing, matrix completion is used to recover a low-rank matrix based on a subset of its entries, requiring only a limited amount of data [33]. Matrix completion involves identifying as closely as possible a low-rank matrix that corresponds to the observed entries of the given incomplete matrix.

Let $\boldsymbol{H} \in \mathbb{R}^{n\times m}$ represents a rank-r noisy and incomplete data matrix with $r \ll \min\{n,m\}$. Assume that some of the matrix entries are given with their indices $(i,j) \in \Upsilon$ are randomly chosen. Thus, observations can be defined by the observation operator $\mathcal{P}_\Upsilon(\boldsymbol{H})$, which has the following definition:

$$[\mathcal{P}_\Upsilon(\boldsymbol{H})]_{ij} = \begin{cases} H_{ij}, & (i,j) \in \Upsilon \\ 0 & \text{otherwise.} \end{cases} \tag{5}$$

In the absence of noise, the original matrix $\boldsymbol{H}$ can be accurately recovered by solving the following optimization problem:

$$\begin{aligned} &\min \ \operatorname{rank}(\boldsymbol{G}) \\ &\text{s.t. } \mathcal{P}_\Upsilon(\boldsymbol{G}) = \mathcal{P}_\Upsilon(\boldsymbol{H}), \end{aligned} \tag{6}$$

where $\operatorname{rank}(\boldsymbol{G})$ represents the rank of the recovered matrix $\boldsymbol{G}$. In (6), the rank minimization involves finding a low-rank matrix $\boldsymbol{G}$ that matches the given entries $H_{i,j}, (i,j) \in \Upsilon$. This optimization problem has a computation complexity that is non-deterministic polynomial-time hard (NP-hard). The nuclear norm, which sums its singular values, can be used to replace the rank, as a convex relaxation. The nuclear norm minimization problem can be described as follows:

$$\begin{aligned} &\min \ \ \|\boldsymbol{G}\|_* \\ &\text{s.t. } \mathcal{P}_\Upsilon(\boldsymbol{G}) = \mathcal{P}_\Upsilon(\boldsymbol{H}), \end{aligned} \tag{7}$$

where $\|\boldsymbol{G}\|_*$ represents the nuclear norm of the matrix $\boldsymbol{G}$. It is defined as

$$\|\boldsymbol{G}\|_* = \sum_{i=1}^{\min\{n,m\}} \sigma_i, \tag{8}$$

where $\sigma_i \geq 0$ is the i-th singular value of the matrix $\boldsymbol{G}$.

A number of research efforts have been conducted on matrix completion to solve (7), including fixed point continuation with approximate singular value decomposition (FPCA) [34], iterative reweighted least squares algorithm (IRLS-M) [35], and singular value thresholding (SVT) [36]. Nuclear-norm minimization methods require singular value decompositions (SVD) of matrices, which are computationally expensive, especially when the underlying matrices have large dimensions and ranks. In this paper, we utilize a low-rank matrix approximation algorithm introduced in [37] that is based on regular QR factorization instead of SVD of the full or partial matrix at each iteration.

C. Problem Formulation

TDOA-based target localization essentially involves the following steps. Initially, packet exchange occurs between anchor nodes and target nodes via a common wireless link. Secondly, we use the collected timestamps to calculate the TDOAs and then estimate the target location. As a result of random transmission delays and packet loss, which reduce the computational accuracy of TDOAs, traditional localization methods are inaccurate.

For accurate and robust localization results, we formulate the target localization problem from noisy and incomplete timestamps into a low-rank matrix recovery problem. We propose a rank-two matrix to hold the collected set of localization timestamps. In the absence of random transmission delays, the formulated timestamp matrix is low-rank. The proposed scheme utilizes this low-rank property to denoise the received timestamps and efficiently recover the lost ones. Then, using the obtained complete and denoised version of the localization timestamps, we can estimate the target location.

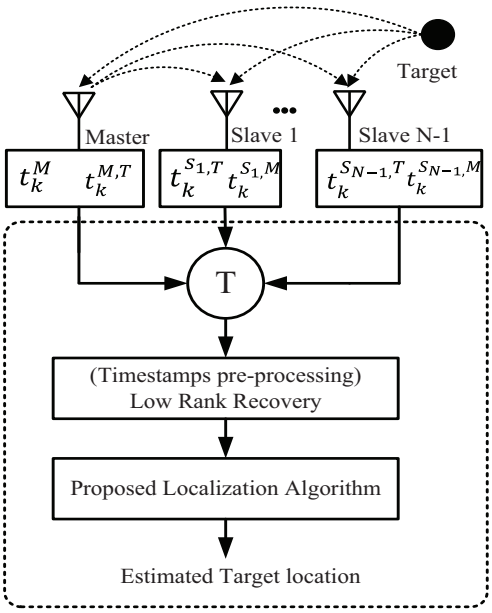

Fig. 4: Proposed robust TDOA measurement scheme.

III. Proposed Matrix Completion based Target Localization

In this section, we present the proposed matrix completion-based indoor localization scheme to get an estimate of the unknown target location from incomplete and noisy timestamps caused by random transmission delays and packet loss. The proposed TDOA-based localization scheme consists of two main stages as shown in Fig. 4.

A. Timestamps Matrix Formulation

Consider a positioning system with one master anchor, $N-1$ slave anchors, and one unknown target node. Once J localization rounds have been completed, we will collect a set of timestamps. In this paper, we propose a matrix formulation for denoising and recovering lost timestamps during the process of exchanging localization packets. The proposed scheme defines a localization timestamp matrix $\boldsymbol{T}_s$ that stores the timestamps collected during the localization rounds. Each row of the localization timestamp matrix $\boldsymbol{T}_s$ represents the localization round for all anchor nodes, while each column represents the localization timestamp for that round. The localization timestamp matrix $\boldsymbol{T}_s$ is defined as follows

$$\boldsymbol{T}_s = \begin{bmatrix} t_1^M & t_1^{S_1,M} & \cdots & t_1^{S_{\mathrm{N}-1},M} & t_1^{M,T} & t_1^{S_1,T} & \cdots & t_1^{S_{\mathrm{N}-1},T} \\ t_2^M & t_2^{S_1,M} & \cdots & t_2^{S_{\mathrm{N}-1},M} & t_2^{M,T} & t_2^{S_1,T} & \cdots & t_2^{S_{\mathrm{N}-1},T} \\ \vdots & \vdots & \ddots & \vdots & \vdots & \vdots & \ddots & \vdots \\ t_J^M & t_J^{S_1,M} & \cdots & t_J^{S_{\mathrm{N}-1},M} & t_J^{M,T} & t_J^{S_1,T} & \cdots & t_J^{S_{\mathrm{N}-1},T} \end{bmatrix}, \tag{9}$$

The symbols in the $\boldsymbol{T}_s$ matrix are defined as follows:

- t_k^M : The start time of each round of timestamp collection, which is periodically initiated by the master anchor sending calibration packets at fixed intervals $\Delta\tau$.
- ${t_k}^{S_i,M}$: The timestamp recorded when the calibration packet was received from the i-th slave anchor.
- ${t_k}^{M,T}$: The timestamp recorded when the localization packet was received from the master anchor.
- ${t_k}^{S_i,T}$: The timestamp recorded when the localization packet was received from the i-th slave anchor.

The target node can be considered stationary for a short period of time. Considering that all anchors are equipped with the same crystals and operate in the same environment, and the master anchor initiates new positioning rounds at very short intervals, timestamps are often tightly correlated without random delays. Ignoring the random transmission delays of anchors, the timestamp matrix $\boldsymbol{T}_s$ can be viewed as elements of the previous row delayed by a fixed time interval $\Delta\tau$. After elementary row transformation, matrix $\boldsymbol{T}_s$ can be transformed into the following:

$$\boldsymbol{T}_s \rightarrow \begin{bmatrix} t_1^M & t_1^{S_1,M} & \cdots & t_1^{S_{\mathrm{N}-1},M} & t_1^{M,T} & t_1^{S_1,T} & \cdots & t_1^{S_{\mathrm{N}-1},T} \\ \Delta\tau & \Delta\tau & \cdots & \Delta\tau & \Delta\tau & \Delta\tau & \cdots & \Delta\tau \\ 0 & 0 & \cdots & 0 & 0 & 0 & \cdots & 0 \\ \vdots & \vdots & \ddots & \vdots & \vdots & \vdots & \ddots & \vdots \\ 0 & 0 & \cdots & 0 & 0 & 0 & \cdots & 0 \end{bmatrix}, \tag{10}$$

Thus, the collected timestamp matrix $\boldsymbol{T}_s$ is a rank-two matrix.

B. Recovery of Localization Timestamps Matrix

Due to hardware failure and wireless channel conditions, some packets may be lost during the localization packet exchange process. In addition, the collected localization timestamps are perturbed by random transmission delays. Thus, some entries of the formulated matrix $\boldsymbol{T}_s$ are missing and the observed ones are corrupted by delays. The observed entries of the timestamp matrix $\boldsymbol{T}_s$ can be defined by the observation operator $\mathcal{P}_\Upsilon[\boldsymbol{T}_s]$, which is given by

$$\mathcal{P}_\Upsilon[\boldsymbol{T}_s(i,j)] = \begin{cases} \boldsymbol{T}_s(i,j), & (i,j) \in \Upsilon \\ 0 & \text{otherwise.} \end{cases} \tag{11}$$

where Υ represents the subset of known entries in the $\boldsymbol{T}_s$ matrix. The noisy incomplete version $\boldsymbol{T}_{s_n}$ of the noise-free timestamp matrix $\boldsymbol{T}_s$ can be written as

$$\boldsymbol{T}_{s_n} = \boldsymbol{T}_s + \boldsymbol{W}, \tag{12}$$

where $\boldsymbol{W}$ defines the noise matrix caused by random transmission delays during the localization packets exchange process. Our aim is to search for a denoised, complete, and low-rank matrix $\hat{\boldsymbol{T}}_s$ from the noisy incomplete matrix $\boldsymbol{T}_{s_n}$ with the observed subset Υ. The proposed scheme exploits the low-rank property of the matrix $\boldsymbol{T}_s$ to recover lost entries through matrix completion theory.

In this subsection, we formulate the indoor localization problem from a noisy and incomplete timestamp matrix as a low-rank matrix completion problem using the subset of observed entries Υ. In this paper, we utilize a low-rank approximation algorithm based on Frobenius norm minimization proposed in [37] to search for the rank-r matrix $\hat{\boldsymbol{T}}_s$. The recovered matrix $\hat{\boldsymbol{T}}_s \in \mathbb{R}^{J\times K}$ can be decomposed into $\hat{\boldsymbol{T}}_s = \boldsymbol{P}\boldsymbol{Q}$, $\boldsymbol{P} \in \mathbb{R}^{J\times r}$ and $\boldsymbol{Q} \in \mathbb{R}^{r\times K}$. Thus, the rank

Algorithm 1 :Low-Rank Matrix Approximation (LRMA) Algorithm

Input: $\boldsymbol{T}_s$

Initialize: $\boldsymbol{P}_0 \in \mathbb{C}^{N\times l}$, $\boldsymbol{Q}_0 \in \mathbb{C}^{l\times K}$, i_{max} = maximum iteration number, $\tau = 10^{-6}$

Repeat

$\mathbf{P}_{i+1} = \mathbf{R}_i\mathbf{Q}_i^{+} = \arg\min_{\mathbf{P}} \frac{1}{2}\left\|\mathbf{R}_i - \mathbf{P}_i\mathbf{Q}_i\right\|_{\mathrm{F}}^2$

$\mathbf{Q}_{i+1} = \mathbf{P}_{i+1}^{+}\mathbf{R}_i = \arg\min_{\mathbf{Q}} \frac{1}{2}\left\|\mathbf{R}_i - \mathbf{P}_{i+1}\mathbf{Q}_i\right\|_{\mathrm{F}}^2$

$i = i + 1$

Until $\frac{\|\mathbf{R}_{i+1}-\mathbf{P}_{i+1}\mathbf{Q}_{i+1}\|_{\mathrm{F}}^2}{\|\mathbf{R}_{i+1}\|_{\mathrm{F}}^2} \le \tau$ **or** $i >= i_{max}$

Onputs: $\hat{\boldsymbol{T}}_s = \mathbf{P}_{i+1}\mathbf{Q}_{i+1}$

minimization problem in (10) can be formulated as a non-convex relaxation given by

$$\begin{aligned} &\min_{\boldsymbol{P},\mathbf{Q},\mathbf{R}} \frac{1}{2}\|\mathbf{R} - \mathbf{P}\mathbf{Q}\|_F^2 \\ &\text{s.t. } P_\Upsilon(\mathbf{R}) = \mathcal{P}_\Upsilon(\boldsymbol{T}_{s_n}), \end{aligned} \tag{13}$$

where $\boldsymbol{R} \in \mathbb{R}^{J\times K}$. In the proposed algorithm, the three variables $\boldsymbol{R}$, $\boldsymbol{P}$, and $\boldsymbol{Q}$ are updated iteratively by minimizing (13) with respect to each of them while the other two are fixed. At the i-iteration, by fixing the variables $\boldsymbol{Q}$ and $\boldsymbol{R}$, we update the variable $\boldsymbol{P}$ as follows:

$$\mathbf{P}_{i+1} = \mathbf{R}_i\mathbf{Q}_i^{+} = \arg\min_{\mathbf{P}} \frac{1}{2}\left\|\mathbf{R}_i - \mathbf{P}_i\mathbf{Q}_i\right\|_{\mathrm{F}}^2 \tag{14}$$

where $\mathbf{Q}_i^{+}$ represents the Moore-Penrose pseudoinverse of matrix $\mathbf{Q}$ at the i-iteration. A similar procedure is followed for updating matrices $\boldsymbol{Q}$ and $\boldsymbol{R}$ using the recent values of the other two fixed matrices. The values of $\mathbf{Q}_i$ and $\mathbf{R}_i$ are given by

$$\begin{aligned} \mathbf{Q}_{i+1} &= \mathbf{P}_{i+1}^{+}\mathbf{R}_i = \arg\min_{\mathbf{Q}} \tfrac{1}{2}\left\|\mathbf{R}_i - \mathbf{P}_{i+1}\mathbf{Q}_i\right\|_{\mathrm{F}}^2 \\ \mathbf{R}_{i+1} &= \mathbf{P}_{i+1}\mathbf{Q}_{i+1} + \mathcal{P}_\Upsilon\left(\mathbf{T}_{s_n} - \mathbf{P}_{i+1}\mathbf{Q}_{i+1}\right). \end{aligned} \tag{15}$$

Here are the criteria for stopping the algorithm:

$$\frac{\left\|\mathbf{R}_{i+1} - \mathbf{P}_{i+1}\mathbf{Q}_{i+1}\right\|_{\mathrm{F}}^2}{\|\mathbf{R}_{i+1}\|_{\mathrm{F}}^2} \le \tau, \tag{16}$$

where τ denotes a small positive constant. Then a complete and denoised low rank matrix is obtained based on $\hat{\boldsymbol{T}}_s = \mathbf{P}_{i+1}\mathbf{Q}_{i+1}$. The low rank recovery algorithm is summarized in **Algorithm 1**.

C. TDOA based Indoor Localization

Once the complete and denoised timestamp matrix $\hat{\boldsymbol{T}}_s$ is recovered, the unknown target location can be estimated using the traditional LS and Chan algorithms.

In a geometric sense, TDOA localization methods are hyperbolic location methods. For each anchor pair, a hyperbola branch can be drawn based on the difference in reception times. The point where all hyperbolas intersect marks the position of the target.

Suppose that the coordinates of the target are expressed as (x, y), and the coordinates of i-th known anchor are expressed as (x_i, y_i), the distance relationship between the target node and each known anchor is given by

$$R_i = \sqrt{(x_i - x)^2 + (y_i - y)^2}. \tag{17}$$

With anchor number 1 as the master anchor, the distance between master anchor and slave anchor is defined by .

$$R_{i,1} = R_i - R_1 = \boldsymbol{v} \times T_k^{M,S_i}, \tag{18}$$

where $\boldsymbol{v}$ is the propagation speed of the anchor nodes, T_k^{M,S_i} A represents the TDOA value of k-th round resulting from equation (4).

Therefore, we can obtain the position of the target (x, y) in the 2D model by using the following TDOA equations for N anchors.

$$\begin{cases} R_{2,1} = \sqrt{(x-x_2)^2 + (y-y_2)^2} - \sqrt{(x-x_1)^2 + (y-y_1)^2} \\ R_{3,1} = \sqrt{(x-x_3)^2 + (y-y_3)^2} - \sqrt{(x-x_1)^2 + (y-y_1)^2} \\ \vdots \\ R_{N,1} = \sqrt{(x-x_N)^2 + (y-y_N)^2} - \sqrt{(x-x_1)^2 + (y-y_1)^2} \end{cases} \tag{19}$$

In this paper, we consider using two typical target location estimation algorithms, i.e. LS algorithm and Chan algorithm [38].

1) LS method: The LS method is the simple and effective method to solve nonlinear hyperbolic equations in (19). After simplifying equation (19), it can be rewritten as

$$x_{i,1}x + y_{i,1}y = -R_{i,1}R_1 + \frac{1}{2}\left(V_i - V_1 - R_{i,1}^2\right), i = 2, 3, \ldots, N \tag{20}$$

where $x_{i,1} = x_i - x_1$, $y_{i,1} = y_i - y_1$, and $V_i = x_i^2 + y_i^2$. Rewrite (20) into matrix form

$$AX = b, \tag{21}$$

where $A = \begin{pmatrix} x_{2,1} & y_{2,1} \\ x_{3,1} & y_{3,1} \\ \vdots & \vdots \\ x_{i,1} & y_{i,1} \end{pmatrix}$, $X = \begin{bmatrix} x \\ y \end{bmatrix}$,

$b = -\left\{ \begin{bmatrix} R_{2,1} \\ R_{3,1} \\ \vdots \\ R_{i,1} \end{bmatrix} R_1 + \frac{1}{2} \begin{bmatrix} R_{2,1}^2 - V_2 + V_1 \\ R_{3,1}^2 - V_3 + V_1 \\ \cdots \\ R_{i,1}^2 - V_i + V_1 \end{bmatrix} \right\}$.

The minimum estimate of X can be obtained by

$$\hat{X} = \left(A^{\mathrm{T}}A\right)^{-1}A^{\mathrm{T}}b. \tag{22}$$

2) Chan method: Suppose that $Z_a = \left[Z_p^T, R_1\right]^T$, where $Z_p = [x, y]^T$ is the position of the target node, the positioning error vector can be represented as

$$\varepsilon = h - G_a Z_a, \tag{23}$$

where $h = \frac{1}{2}\begin{bmatrix} {R_{2,1}}^2 - V_2 + V_1 \\ {R_{3,1}}^2 - V_3 + V_1 \\ \vdots \\ {R_{i,1}}^2 - V_i + V_1 \end{bmatrix}$, $G_a = -\begin{bmatrix} x_{2,1} & y_{2,1} & R_{2,1} \\ x_{3,1} & y_{3,1} & R_{3,1} \\ & \vdots & \\ x_{i,1} & y_{i,1} & R_{i,1} \end{bmatrix}$.

Assuming that the variance of the TDOA measurements is $\sigma_{i,1}$, the measurement error covariance matrix U is expressed as

$$U = \mathrm{diag}\left\{ \begin{array}{cccc} \sigma_{2,1}^2 & \sigma_{3,1}^2 & \cdots & \sigma_{i,1}^2 \end{array} \right\}. \tag{24}$$

When the measurement error of TDOA is relatively small, the covariance matrix of the error vector can be approximated by

$$\Psi = E\left[\varepsilon\varepsilon^T\right] = c^2 BUB, \tag{25}$$

where $B = \mathrm{diag}\left\{ \begin{array}{cccc} R_2^0 & R_3^0 & \cdots & R_i^0 \end{array} \right\}$. In general, the approximate coordinate (x, y) of the target obtained by WLS can calculate R_i, and replace R_i^0 with R_i, then the approximate coordinate of the target node $Z_a = [x^0, y^0, R_1^0]^T$ can be expressed as

$$Z_a = \left(G_a^T \Psi^{-1} G_a\right)^{-1} G_a^T \Psi^{-1} h. \tag{26}$$

To improve accuracy, Z_a' is estimated with WLS. That is:

$$\varepsilon' = h' - G_a' Z_a', \tag{27}$$

where $h' = \begin{bmatrix} \left(x^0 - x_1\right)^2 \\ \left(y^0 - y_1\right)^2 \\ R_1^{0^2} \end{bmatrix}, G_a' = \begin{bmatrix} 1 & 0 \\ 0 & 1 \\ 1 & 1 \end{bmatrix}$,

$Z_a' = \begin{bmatrix} (x - x_1)^2 \\ (y - y_1)^2 \end{bmatrix}$. The covariance matrix Ψ' can be expressed as

$$\Psi' = E\left[\varepsilon'\varepsilon'^T\right] = 4B'\left(G_a'^T \Psi' G_a'\right)^{-1} B', \tag{28}$$

where $B' = \mathrm{diag}\left\{ \begin{array}{ccc} x^0 - x_1 & y^0 - y_1 & R_1^0 \end{array} \right\}$. Z_a' can be obtained by

$$Z_a' = \left(G_a'^T \Psi'^{-1} G_a'\right)^{-1} G_a'^T \Psi'^{-1} h'. \tag{29}$$

The final result is expressed as

$$Z_p = \pm\sqrt{Z_a'} + \left[\begin{array}{cc} x_1 & y_1 \end{array} \right]^{-1} \tag{30}$$

To ascertain the covariance matrix of position estimates, we define $x = x^0 + e_x$ and $y = y^0 + e_y$ within the domain z_p, where the errors e_x and e_y are relatively small in comparison to x^0 and y^0. Based on (25) and (28), the corresponding position covariance matrix Z_p is determined as follows:

$$\Phi = \mathrm{cov}\left(Z_p\right) = \frac{1}{4} B''^{-1} \mathrm{cov}\left(Z_a'\right) B''^{-1}, \tag{31}$$

where $B'' = \begin{bmatrix} \left(x^0 - x_1\right) & 0 \\ 0 & \left(y^0 - y_1\right) \end{bmatrix}$. The covariance matrix of Z_a' can be expressed as [39]

$$\mathrm{cov}\left(\mathbf{Z}_a'\right) = \left(G_a'^T \Psi'^{-1} G_a'\right)^{-1}. \tag{32}$$

Upon using (25), (28) and (32), (31) is found to be

$$\Phi = c^2 B'' G_a'^T B'^{-1} G_a^T B^{-1} U^{-1} B^{-1} G_a B'^{-1} G_a' B''\Big)^{-1}. \tag{33}$$

The Cramer-Rao lower bound (CRLB) of the estimated target's coordinates can be obtained by [39]

$$\Phi = c^2 \left(G_t^T U^{-1} G_t\right)^{-1}, \tag{34}$$

where $G_t = \begin{bmatrix} \tilde{x}_1/{R_1}^0 - \tilde{x}_2/{R_2}^0 & \tilde{y}_1/{R_1}^0 - \tilde{y}_2/{R_2}^0 \\ \tilde{x}_1/{R_1}^0 - \tilde{x}_3/{R_3}^0 & \tilde{y}_1/{R_1}^0 - \tilde{y}_3/{R_3}^0 \\ \\ \tilde{x}_1/{R_1}^0 - \tilde{x}_M/{R_M}^0 & \tilde{y}_1/{R_1}^0 - \tilde{y}_M/{R_M}^0 \end{bmatrix}$,

$\tilde{x}_i = x_i - x^0$, $\tilde{y}_i = y_i - y^0$, $i = 1, 2, ..., M$, ${R_i}^0$ is defind in (17) with $(x, y) = (x^0, y^0)$. In our experiment, we will use the recovered timestamp matrix as $\hat{\boldsymbol{T}}_s$ to calculate U.

The traditional LS and Chan algorithms rely upon accurate and sufficient distance measurements. Distance measurements are subject to noise and data loss, so the above methods are insufficiently precise when the distance information is incomplete or damaged.

IV. Proposed Linear Fusion Target Localization

In this subsection, we use the information obtained from multiple localization rounds to improve the accuracy of target localization. For the purpose of determining the final location of the target, we devise a data fusion strategy. Based on linear information fusion, the final estimate of target location is given by

$$\hat{A} = \alpha_1 \hat{A}_1 + \alpha_2 \hat{A}_2 + \cdots + \alpha_{J-1} \hat{A}_{J-1} = \sum_{j=1}^{J-1} \alpha_j \hat{A}_j, \tag{35}$$

where $\hat{A}_j, j = 1, 2, \ldots, J-1$ refer to the $J-1$ target location estimators which are based on different localization rounds, and α_j is the weighing factor of j-th location estimator. Our objective is to optimize the final result by estimating the weighting factors $\{\alpha_j\}_{j=1}^{J-1}$ using the weighted linear minimum variance information fusion algorithm. In the proposed algorithm, we determine the weighting factors by comparing the deviation of each location estimator from the mean of all location estimators. The larger the deviation, the smaller the corresponding weight should be. Let the fusion estimation error be

$$\widetilde{A}_j = A - \hat{A}_j,\ j = 1, 2, \ldots, J-1, \tag{36}$$

where A represents the mean of the location estimators $\left\{\hat{A}_j\right\}_{j=1}^{J-1}$. Considering $\hat{A}_j$ is unbiased, then $\mathbf{E}[\hat{A}_j] = A$. By taking the mathematical expectation of the fusion estimator $\hat{A}$ in (43)

$$\mathbf{E}[\hat{A}] = \mathbf{E}[\sum_{j=1}^{J-1} \alpha_j \hat{A}_j] = \sum_{j=1}^{J-1} \alpha_j \mathbf{E}[\hat{A}_j] = \sum_{j=1}^{J-1} \alpha_j A = A. \tag{37}$$

Then,

$$\sum_{j=1}^{J-1} \alpha_j = 1. \tag{38}$$

Algorithm 2 :Proposed Linear Fusion (LF) Algorithm

1: **Input:** $Anchors = (x_i, y_i), target = (x_0, y_0)$

2: In each timestamp sampling cycle, the master anchor node initiates calibration packets for $\boldsymbol{J}$ rounds.

3: Collect timestamps recorded by each anchor node $\left\{t_k^M, t_k^{S_1,M}, \ldots, t_k^{S_{N-1},M}, t_k^{M,T}, t_k^{S_1,T}, \ldots, t_k^{S_{N-1},T}\right\}_{k=1}^{J}$.

4: Form the timestamps matrix $\boldsymbol{T}_{s_n}$ from the successfully recorded timestamps and save the coordinates of the known entries into the index set Υ.

5: Find an estimate of the complete denoised low rank matrix $\hat{\boldsymbol{T}}_s$ by solving (13).

6: Calculate the TDOA values $\{T_k^{M,S_i}\}_{k=1}^{J-1}$ from (3) and (4) using the recovered timestamps matrix $\hat{\boldsymbol{T}}_s$.

7: Use the calculated TDOA values $\{T_k^{M,S_i}\}_{k=1}^{J-1}$ to estimate the positions of target node $\{\hat{A}_j\}_{j=1}^{J-1}$ based on traditional LS method and traditional Chan method mentioned in section III.

8: Estimate the weights $\{\alpha_j\}_{j=1}^{J-1}$ by (42) to optimize the final position $\hat{A}$:

$$\hat{A} = \sum_{j=1}^{J-1} \alpha_j \hat{A}_j.$$

9: **O**utput:Estimatd target $= (x, y)$

The mean square error Ω of the fusion location estimator $\hat{A}$ is given by

$$\begin{aligned}\Omega(\hat{A}) &= \mathbf{E}\left[(\hat{A}-A)^T(\hat{A}-A)\right] \\ &= \mathbf{E}\left[\sum_{j=1}^{J-1}\alpha_j(\hat{A}_j-A)^T(\hat{A}_j-A)\right] \\ &+ \mathbf{E}\left[2\sum_{j=1,i=1,j\neq i}^{J-1}\alpha_j\alpha_i(\hat{A}_j-A)^T(\hat{A}_i-A)\right].\end{aligned} \tag{39}$$

It is usually reasonable to assume that different estimators are independent. Thus, $\hat{A}_1, \hat{A}_2, \cdots, \hat{A}_J =$ are assumed to be independent of each other. Hence, $\mathbf{E}\left[(\hat{A}_j - A)^T(\hat{A}_i - A)\right] = 0$. The simplified form of (39) is given as

$$\begin{aligned}\Omega(\hat{A}) &= \mathbf{E}\left[\sum_{j=1}^{J-1}\alpha_j(\hat{A}_j-A)^T(\hat{A}_j-A)\right] \\ &= \sum_{j=1}^{J-1}\alpha_j\Omega(\hat{A}_j).\end{aligned} \tag{40}$$

According to the [40], the optimal weight is to minimize $\Omega(\hat{A})$ under the constraint (38). Constructing the objective function using the Lagrange multiplier method, we get

$$\min_{\alpha_j(j=1,2,\cdots,J-1)} F = \sum_{j=1}^{J-1}\alpha_j^2\Omega\left(\hat{A}_j\right) + \lambda\left(\sum_{i=1}^{J-1}\alpha_j - 1\right) \tag{41}$$

TABLE I: Simulation Parameters.

Parameter	Description	Value
J	The number of rounds	[10, 20]
N	The number of localization anchors	5
SNR	Standard deviation of random delay	[5,15]
$loss$	Ratio of packet loss	10%

Then, the optimal weighting factors $\{\alpha_j\}_{j=1}^{J-1}$ are given by

$$\alpha_j = \frac{1}{\Omega(\hat{A}_j)}\left(\sum_{j=1}^{J-1}\frac{1}{\Omega(\hat{A}_j)}\right)^{-1} \tag{42}$$

Hence, the fusion location estimator is calculated as

$$\hat{A} = \sum_{j=1}^{J-1}\left[\frac{1}{\Omega(\hat{A}_j)}\left(\sum_{j=1}^{J-1}\frac{1}{\Omega(\hat{A}_j)}\right)^{-1} \times A_j\right]. \tag{43}$$

Based on (43), the final estimate of tag location is obtained using different localization rounds. The proposed linear fusion indoor localization algorithm is summarized in **Algorithm 2**.

V. Simulation Results

In this section, we evaluate the performance of the LF algorithm for indoor target location estimation in the presence of packet loss and random transmission delays.

A. Simulation Setup

In all experiments, the localization system model consists of five anchor nodes, i.e. one master anchor, four slave anchors, and one randomly positioned static target. We set the signal-to-noise ratios SNR $\in [5, 15]$, and the propagation speed $\boldsymbol{v}$ of the sensors to $3 \times 10^7 m/s$. The random delays are normally distributed with zero mean $\mu = 0$ and variance $\sigma_n^2 = 10\ \hat{}\ (-(SNR)/10)/\boldsymbol{v}$. It is assumed that the standard deviation of the noise is the same for all anchor nodes. The experimental parameters are listed in Table I. We consider the root-mean-squared error (RMSE) and the cumulative distribution function (CDF) as performance metrics to measure the accuracy of the estimated target location.

B. Localization Performance with The Proposed Low Rank Matrix Recovery

In this subsection, we study the performance of the proposed algorithm in terms of RMSE and CDF in the presence of packet loss and transmission delays. The performance is examined for a packet loss ratio of 10%.

In Fig. 5, we evaluate the denoise performance of low-rank matrix approximation. We compare the RMSE and SNR of target positions estimated with and without LRMA estimators in the presence of normal distribution transmission delays. It is observed that the LRMA estimators significantly improve target localization accuracy, especially at low SNR compared to the existing LS and Chan algorithms. Note that the performance of the proposed LRMA algorithm is close to the CRLB

This article has been accepted for publication in IEEE Internet of Things Journal. This is the author's version which has not been fully edited and content may change prior to final publication. Citation information: DOI 10.1109/JIOT.2023.3327883

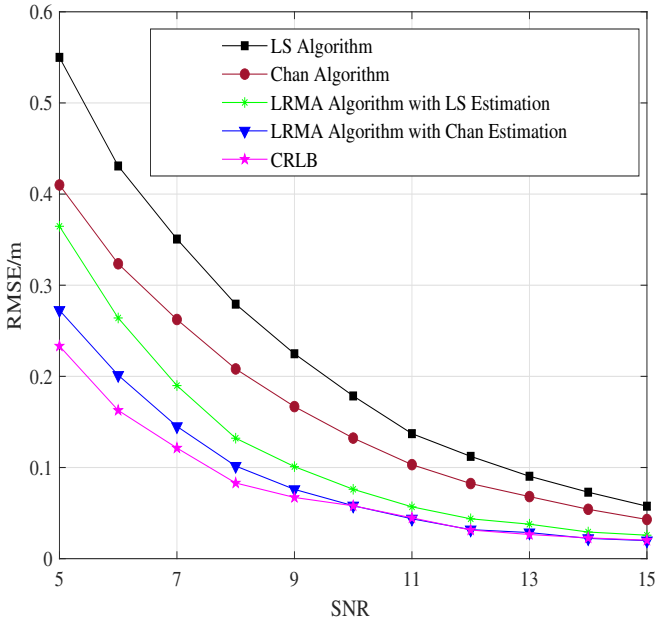

Fig. 5: RMSE of the estimated location v.s. SNR.

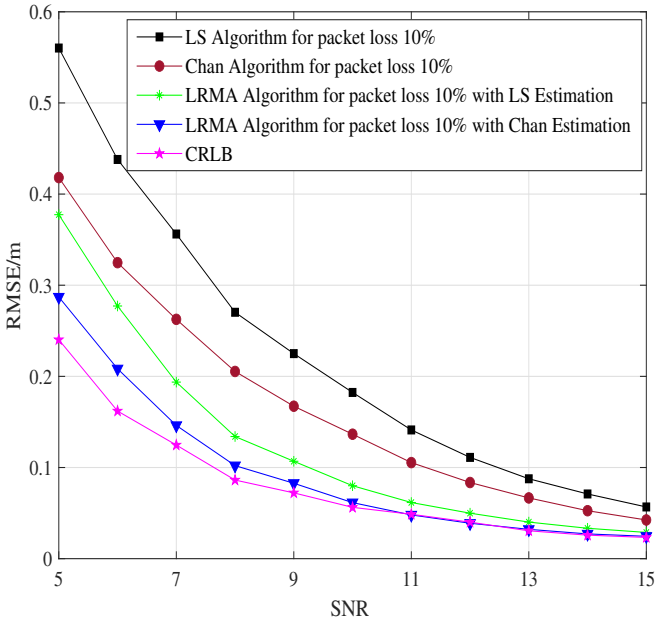

Fig. 6: RMSE of the estimated location with packet loss v.s. SNR.

and the proposed algorithm with CHAN estimation curve is merging with the CRLB curve for SNR ≥ 10 dB.

In Fig. 6, we evaluate the recovery performance of low-rank matrix approximation. Considering packet loss, we compare the RMSE and SNR of target positions estimated using and without LRMA estimators. The addition of LRMA estimators improves target localization accuracy significantly, especially at low SNR, in comparison with the existing LS and Chan algorithms.

C. Localization Performance with The Proposed Linear Fusion Algorithm

In this subsection, we study the localization performance with the proposed linear fusion algorithm (LF). In following figures, LF algorithm refers to the proposed algorithm including low rank matrix recovery and the proposed linear fusion strategy.

In Fig. 5 and Fig. 6, the positioning results from multiple localization rounds are averaged to get the final target's position. In the proposed fusion strategy, less weights are given to poor positioning results, whereas the larger weight are given to the good ones to improve the accuracy of target localization.

In Fig. 7, we compare the RMSE of estimated target locations versus SNR using different approaches in the presence of normally distributed transmission delays. It is observed that the proposed algorithm significantly improves target localization accuracy, especially at low SNR compared to the existing LS and Chan algorithms. The reason for this is that the LF algorithm, in addition to the proposed fusion method, corrects the collected localization timestamps first. In contrast, the LS and Chan algorithms use the collected timestamp values directly.

Fig. 8 shows the CDF of localization errors for the proposed algorithm and other algorithms with SNR set to 10. It shows that the CDF of the proposed scheme is much higher than the traditional LS and Chan methods. With the timestamps

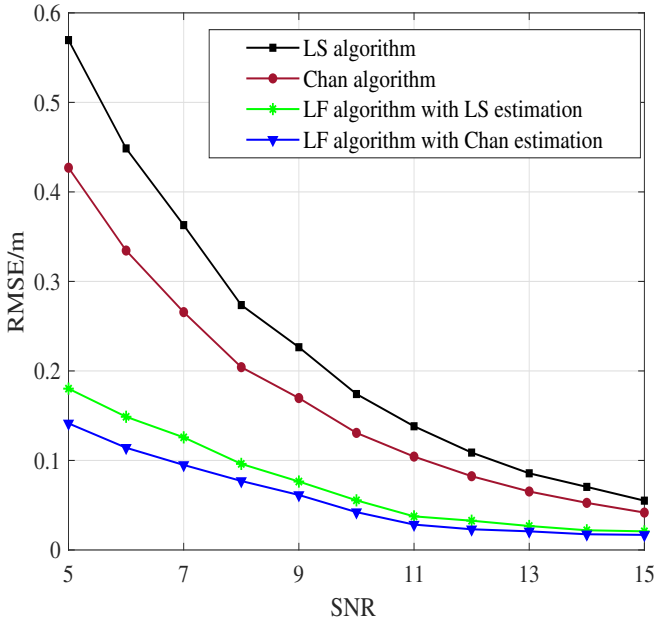

Fig. 7: RMSE of the estimated location v.s. SNR.

correction, the distance error of the LF algorithm with Chan estimation is less than 0.08 m, accounting for approximately 95% of all times, and that of the LF algorithm with LS estimation is less than 0.11 m, accounting for about 95% of all times. While, the distance errors of existing Chan and LS methods are less than 0.18 m and 0.24 m, respectively, with a probability of approximately 95%. It can be concluded that the average distance error reduces from 0.18 m and 0.24 m to 0.08 m and 0.11 m, with a relative performance improvement of around 55%.

Moreover, Fig. 9 illustrates the RMSE versus the number of localization rounds J, where the SNR is set to 10. The results show that the proposed scheme can estimate the target position efficiently under random transmission delays even with a small number of localization rounds. In addition, it is clear that the proposed algorithm can benefit from extra positioning

This article has been accepted for publication in IEEE Internet of Things Journal. This is the author's version which has not been fully edited and content may change prior to final publication. Citation information: DOI 10.1109/JIOT.2023.3327883

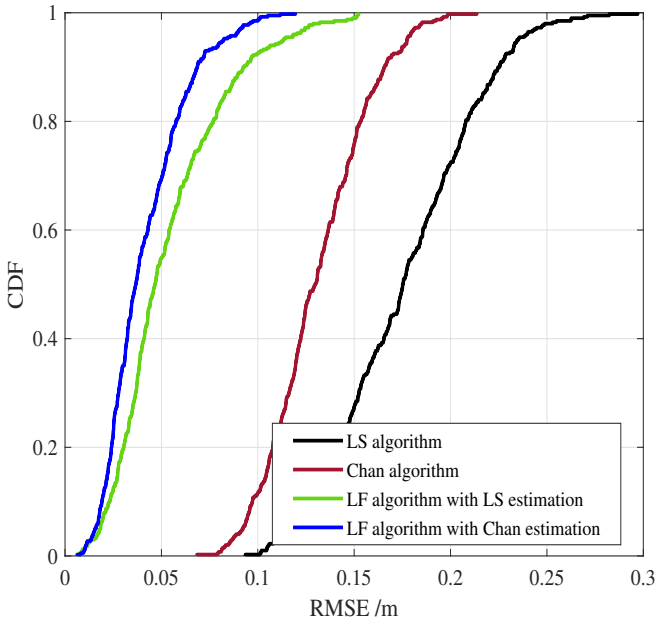

Fig. 8: CDF of the estimated location.

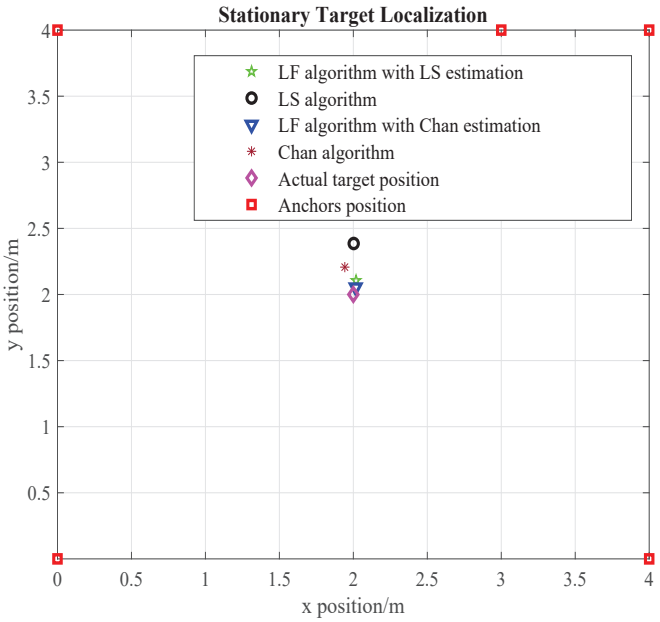

Fig. 10: Localization results under the interference of mixed noise.

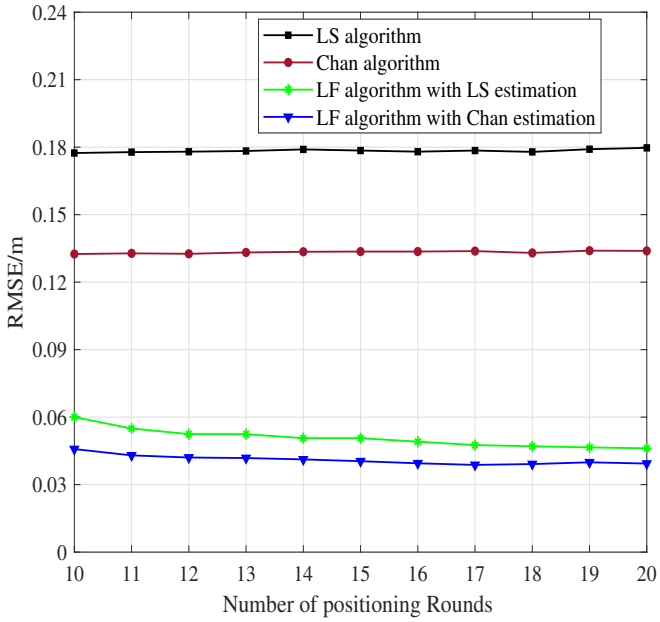

Fig. 9: RMSE of the estimated location v.s. the number of positioning rounds.

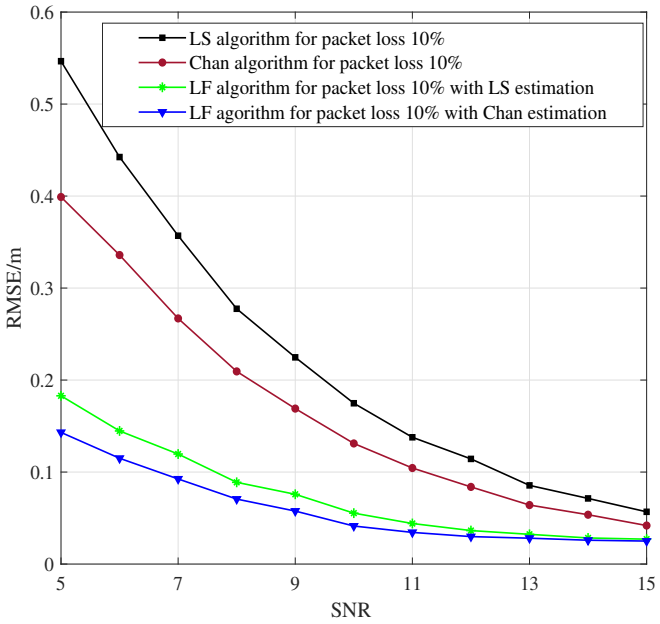

Fig. 11: RMSE of the estimated location with packet loss v.s. SNR.

rounds to improve target position estimation accuracy, while traditional methods have approximately constant behavior with position rounds.

Fig. 10 visualizes the localization results of the target node for a 2-D network. We compare the true target position with the position estimates obtained using different approaches. The obtained results show that the proposed algorithm significantly improves the estimation accuracy of target localization. In contrast, traditional LS and Chan methods have poorer performance than the proposed algorithm, and there is a large deviation from the actual position.

In Fig. 11, we show the RMSE of the estimated target location with respect to the SNR under the effect of a packet loss ratio of 10%. The figure illustrates how the performance of the traditional LS and Chan methods degrades when packet loss occurs. It is observed that the proposed matrix completion based localization scheme significantly improves target position estimation accuracy compared with the existing LS and Chan methods. The reason is that the proposed scheme uses recovered timestamps to estimate the target position, in addition to fusing the results obtained from multiple rounds of localization.

From Fig. 11, it is also noticed that the improvement of the proposed target location estimation scheme is superior to the existing methods, especially in severe channel conditions, i.e., low SNR.

Fig. 12 shows the CDF of localization errors of the proposed scheme under the effect of packet loss ratio $= 10\%$. From Fig. 12, we can get the same conclusion, where we can see clearly that the target position estimation based on the proposed matrix completion based scheme performs better than the existing methods. It is observed that the distance

This article has been accepted for publication in IEEE Internet of Things Journal. This is the author's version which has not been fully edited and content may change prior to final publication. Citation information: DOI 10.1109/JIOT.2023.3327883

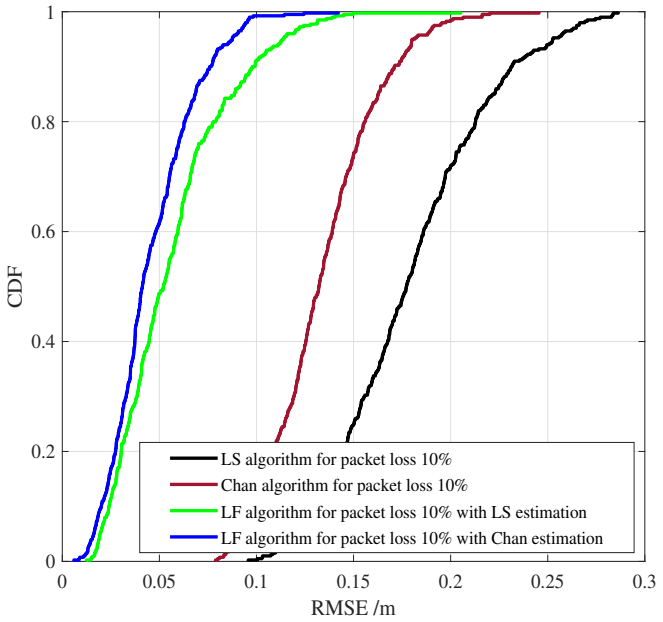

Fig. 12: CDF of the estimated location with packet loss.

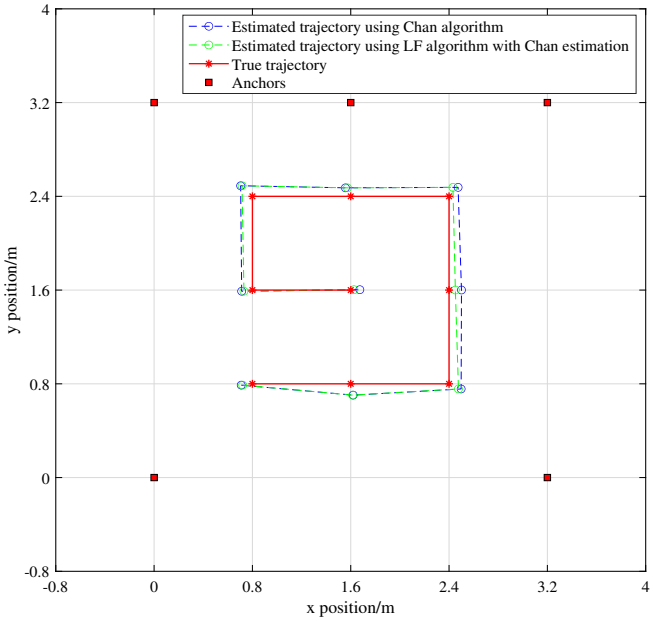

Fig. 13: Experiment of localization trajectory.

errors of the proposed scheme with LS and Chan estimations are less than 0.12 m and 0.09 m, respectively, about 95% of the time. While, the distance errors of the existing LS and Chan methods are less than 0.18 m and 0.25 m, respectively, about 95% of the time. This is due to the denoising feature of the LF localization scheme in addition to the recovery of lost localization timestamps.

The proposed scheme has two stages, the timestaps preprocessing stage and the target position estimation stage. The computational complexity of the estimation stage is the same as that of the traditional LS and CHAN algorithms with order $\mathcal{O}(N^3)$. The timestamps preprocessing stage includes low-rank matrix recovery with complexity $\mathcal{O}(KLog(K)Nr)$ for the timestamps matrix $\boldsymbol{T}_s \in \mathbb{R}^{N\times K}$ with rank r. Thus, the proposed scheme has improved performance compared to existing estimators at slightly higher computational complexity, reduced SNR, and reduced number of packet transmissions for more accurate estimation.

VI. Experimental Results

In this section, for an experimentation-based demonstration, we provide experimental results in an indoor environment to validate the performance of the proposed algorithm. First, we describe the experimental setup, followed by the results and discussion.

A. Experimental Setup

As shown in Fig. 12 (a), we use UWB devices as RF front-end modules for localization. The UWB device uses the Decave DWM1000 chip as the transceiver module and the STM32F103C8T6 chip as the control chip, which can be defined as an anchor or target.

The experimental setup is shown in Fig. 12 (b), (c) with an indoor environment consisting of a master anchor, i.e., anchor 1, four slave anchors, a target node, and a personal computer (PC).

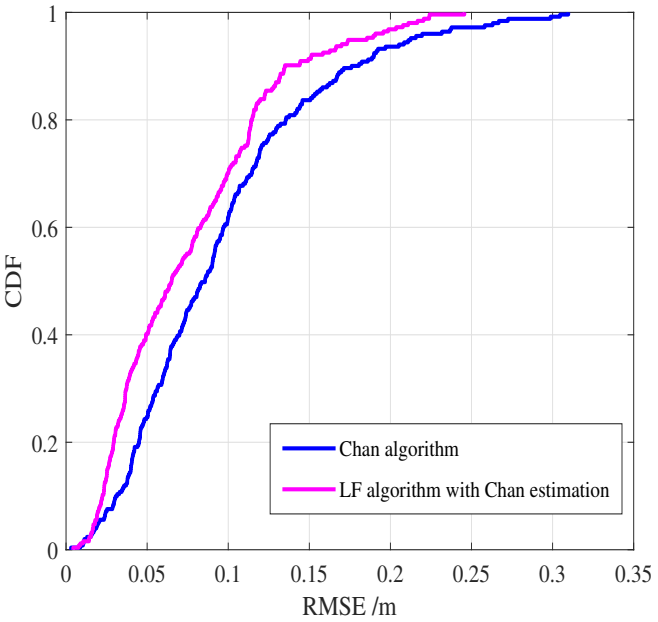

Fig. 14: Localization error CDF.

First, the algorithm initiates the localization process by sending a command to the master anchor. Through the localization process, each slave anchor stores the timestamp data and transmits it back to master anchor 1. To calculate the target location, the master anchor sends the timestamp information to the PC.

B. Experimental Analysis

In the following experiment, we designed the movement track of the target to stay at the same height and move in a square with 2.4 m on each side. Fig. 13. shows the spiral localization of a target node in a 2-D network. For comparison, we compare the trajectory formed by the actual

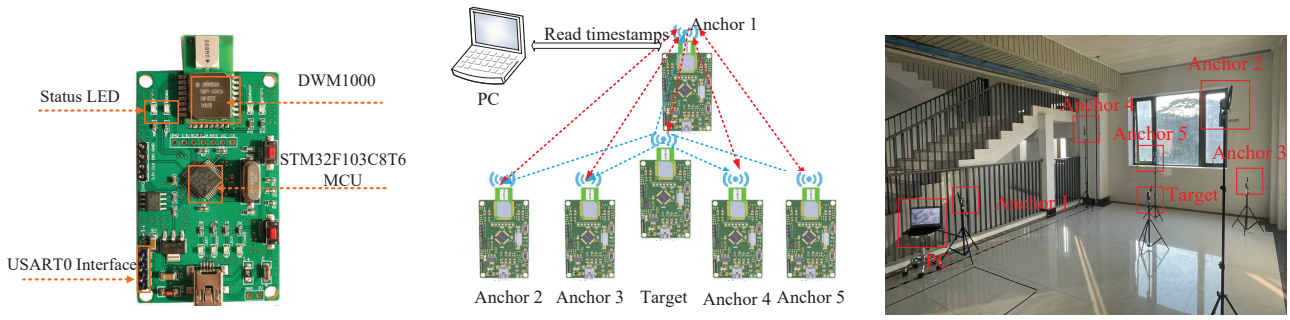

(a) Hardware device of the localization module. (b) Experiental setup for localization (c) Experiental environment

Fig. 15: Indoor localization experiment.

target position with the trajectory estimates obtained using the proposed algorithm and other approaches. Similarly to simulation results, one can see that the proposed scheme with matrix completion and linear fusion achieves better estimation performance of target location than other schemes. The RMSE of target coordinates based on the Chan algorithm is 10.05 cm, and that of target coordinates using the LF algorithm is 8.01 cm.

In Fig. 14, we show the CDF results of the localization error. Obviously, the proposed algorithm performs better than the existing Chan algorithm. It is observed that the distance errors of the proposed scheme with Chan estimations are less than 0.15 m, about 90% of the time. While, the distance errors of the existing Chan methods are less than 0.20 m, about 90% of the time. The reason is that the LF algorithm recovers the lost timestamps and uses them along with the collected values to estimate the target location, whereas the Chan algorithm scheme only uses the collected values.

VII. Conclusion

This paper proposes a robust indoor target location estimation method using the ASync-TDOA localization model with low-rank matrix completion. In the proposed scheme, the localization timestamp correction and completion problem is formulated as a low-rank matrix completion problem, and then the TDOA measurements are calculated from the recovered timestamps. The target location is estimated by the proposed linear fusion strategy based on different localization rounds to further refine the location estimate. In order to verify the effectiveness of the proposed method, numerical simulations were conducted under different SNR values and localization rounds with packet loss and transmission delays. The conducted simulations and experiments illustrate that the proposed scheme outperforms traditional localization methods and achieves higher localization accuracy when transmission delays or packet loss occur.

References

[1] L. M. Borges, F. J. Velez, and A. S. Lebres, "Survey on the characterization and classification of wireless sensor network applications," *IEEE Commun. Surveys Tuts*, vol. 16, no. 4, pp. 1860–1890, 2014.

[2] F. Zafari, A. Gkelias, and K. K. Leung, "A survey of indoor localization systems and technologies," *IEEE Commun. Surveys Tuts*, vol. 21, no. 3, pp. 2568–2599, 2019.

[3] P. S. Farahsari, A. Farahzadi, J. Rezazadeh, and A. Bagheri, "A survey on indoor positioning systems for iot-based applications," *IEEE Internet of Things Journal*, vol. 9, no. 10, pp. 7680–7699, 2022.

[4] H. Obeidat, W. Shuaieb, O. Obeidat, and R. Abd-Alhameed, "A review of indoor localization techniques and wireless technologies," *Wireless Personal Communications*, vol. 119, no. 1, pp. 289–327, Jul 2021.

[5] Y. Xu, Y. S. Shmaliy, Y. Li, and X. Chen, "UWB-based indoor human localization with time-delayed data using efir filtering," *IEEE Access*, vol. 5, pp. 16 676–16 683, 2017.

[6] A. R. Jiménez Ruiz and F. Seco Granja, "Comparing ubisense, bespoon, and decawave UWB location systems: Indoor performance analysis," *IEEE Trans. Instrum. Meas*, vol. 66, no. 8, pp. 2106–2117, 2017.

[7] G. Wang, A. M.-C. So, and Y. Li, "Robust convex approximation methods for TDOA-based localization under nlos conditions," *IEEE Trans. Signal Process* , vol. 64, no. 13, pp. 3281–3296, 2016.

[8] A. Tahat, G. Kaddoum, S. Yousefi, S. Valaee, and F. Gagnon, "A look at the recent wireless positioning techniques with a focus on algorithms for moving receivers," *IEEE Access*, vol. 4, pp. 6652–6680, 2016.

[9] K. Yang, J. An, X. Bu, and G. Sun, "Constrained total least-squares location algorithm using time-difference-of-arrival measurements," *IEEE Trans. Veh. Technol*, vol. 59, no. 3, pp. 1558–1562, 2010.

[10] M. R. Gholami, S. Gezici, and E. G. Strom, "TDOA based positioning in the presence of unknown clock skew," *IEEE Trans. Commun*, vol. 61, no. 6, pp. 2522–2534, 2013.

[11] O. Elnahas, Y. Ma, Y. Jiang, and Z. Quan, "Clock synchronization in wireless networks using matrix completion-based maximum likelihood estimation," *IEEE Trans. Wireless Commun*, vol. 19, no. 12, pp. 8220–8231, 2020.

[12] H. Wang, L. Shao, M. Li, and B. Wang, "A global clock skew estimation scheme for hierarchical wireless sensor networks," *IEEE Access*, vol. 5, pp. 20 333–20 338, 2017.

[13] A. Canclini, F. Antonacci, A. Sarti, and S. Tubaro, "Acoustic source localization with distributed asynchronous microphone networks," *IEEE/ACM Trans. Audio, Speech, Language Process*, vol. 21, no. 2, pp. 439–443, 2013.

[14] B. Xu, G. Sun, R. Yu, and Z. Yang, "High-accuracy TDOA-based localization without time synchronization," *IEEE Trans. Parallel Distrib. Syst*, vol. 24, no. 8, pp. 1567–1576, 2013.

[15] Y. Wang, X. Ma, and G. Leus, "Robust time-based localization for asynchronous networks," *IEEE Trans. Signal Process*, vol. 59, no. 9, pp. 4397–4410, 2011.

[16] Y. Xue, W. Su, H. Wang, D. Yang, and J. Ma, "A model on indoor localization system based on the time difference without synchronization," *IEEE Access*, vol. 6, pp. 34 179–34 189, 2018.

[17] K. C. Ho, X. Lu, and L. Kovavisaruch, "Source localization using tdoa and fdoa measurements in the presence of receiver location errors: Analysis and solution," *IEEE Trans. Signal Process*, vol. 55, no. 2, pp. 684–696, 2007.

[18] K. C. Ho and L. Yang, "On the use of a calibration emitter for source localization in the presence of sensor position uncertainty," *IEEE Trans. Signal Process*, vol. 56, no. 12, pp. 5758–5772, 2008.

[19] A. Vashistha and C. L. Law, "E-DTDOA based localization for wireless sensor networks with clock drift compensation," *IEEE Sensors J*, vol. 20, no. 5, pp. 2648–2658, 2020.

[20] H. H. Fan and C. Yan, "Asynchronous differential TDOA for sensor self-localization," in *2007 IEEE International Conference on Acoustics, Speech and Signal Processing - ICASSP '07*, vol. 2, 2007, pp. II–1109–II–1112.

[21] S. Shojaee, J. Schmitz, R. Mathar, and S. Toledo, "On the accuracy of passive hyperbolic localization in the presence of clock drift," in *2017 IEEE 28th Annual International Symposium on Personal, Indoor, and Mobile Radio Communications (PIMRC)*, 2017, pp. 1–6.

[22] J. Tiemann, F. Eckermann, and C. Wietfeld, "Multi-user interference and wireless clock synchronization in TDOA-based uwb localization," in *2016 International Conference on Indoor Positioning and Indoor Navigation (IPIN)*, 2016, pp. 1–6.

[23] Z. Yang, X. Zhu, W. Yang, and Z. Zhao, "Wireless synchronized uwb tdoa positioning system based on ieee 802.15.4z," in *2021 International Applied Computational Electromagnetics Society (ACES-China) Symposium*, 2021, pp. 1–2.

[24] R. Exel, G. Gaderer, and P. Loschmidt, "Localisation of wireless lan nodes using accurate TDOA measurements," in *2010 IEEE Wireless Communication and Networking Conference*, 2010, pp. 1–6.

[25] N. M. Senevirathna, O. De Silva, G. K. I. Mann, and R. G. Gosine, "Asymptotic gradient clock synchronization in wireless sensor networks for uwb localization," *IEEE Sens. J*, vol. 22, no. 24, pp. 24 578–24 592, 2022.

[26] X. Ouyang, S. Yao, and Q. Wan, "A coherent integrated tdoa estimation method for target and reference signals," *Electronics*, vol. 11, no. 16, 2022.

[27] B. Xu, G. Sun, R. Yu, and Z. Yang, "High-accuracy tdoa-based localization without time synchronization," *IEEE Trans. Parallel Distrib. Syst*, vol. 24, no. 8, pp. 1567–1576, 2013.

[28] S. Kim and J.-W. Chong, "An efficient TDOA-based localization algorithm without synchronization between base stations," *International Journal of Distributed Sensor Networks*, vol. 11, no. 9, p. 832351, 2015.

[29] D. Chiasson, Y. Lin, M. Kok, and P. B. Shull, "Asynchronous hyperbolic uwb source-localization and self-localization for indoor tracking and navigation," *IEEE Internet Things J*, vol. 10, no. 13, pp. 11 655–11 668, 2023.

[30] J. J. Pérez-Solano, S. Ezpeleta, and J. M. Claver, "Indoor localization using time difference of arrival with uwb signals and unsynchronized devices," *Ad Hoc Networks*, vol. 99, p. 102067, 2020.

[31] F. Bandiera, A. Coluccia, G. Ricci, F. Ricciato, and D. Spano, "TDOA localization in asynchronous wsns," in *2014 12th IEEE International Conference on Embedded and Ubiquitous Computing*, 2014, pp. 193–196.

[32] X. Hui, Z. Chen, W. An, and B. Yang, "Robust TDOA localization algorithm for asynchronous wireless sensor networks," *International Journal of Distributed Sensor Networks*, vol. 2015, pp. 1–10, 05 2015.

[33] R. Ma, N. Barzigar, A. Roozgard, and S. Cheng, "Decomposition approach for low-rank matrix completion and its applications," *IEEE Trans. Signal Process*, vol. 62, no. 7, pp. 1671–1683, 2014.

[34] S. Ma, D. Goldfarb, and L. Chen, "Fixed point and bregman iterative methods for matrix rank minimization," *Mathematical Programming*, vol. 128, 05 2009.

[35] M. Fornasier, H. Rauhut, and R. Ward, "Low-rank matrix recovery via iteratively reweighted least squares minimization," *SIAM Journal on Optimization*, vol. 21, 10 2010.

[36] J.-F. Cai, E. Candès, and Z. Shen, "A singular value thresholding algorithm for matrix completion," *SIAM Journal on Optimization*, vol. 20, pp. 1956–1982, 03 2010.

[37] Z. Wen, W. Yin, and Y. Zhang, "Solving a low-rank factorization model for matrix completion by a nonlinear successive over-relaxation algorithm," *Mathematical Programming Computation*, vol. 4, no. 4, pp. 333–361, 2012.

[38] Y. Cheng and T. Zhou, "UWB indoor positioning algorithm based on TDOA technology," in *2019 10th international conference on information technology in medicine and education (ITME)*. IEEE, 2019, pp. 777–782.

[39] Y. T. Chan and K. C. Ho, "A simple and efficient estimator for hyperbolic location," *IEEE Trans. Signal Process*, vol. 42, no. 8, pp. P.1905–1915, 1994.

[40] Z. Deng and R. Qi, "Multi-sensor information fusion suboptimal steady-state kalman filter," *Chinese Science Abstracts*, vol. 6, pp. 183–184, 01 2000.